Ultraviolet Photochemistry of Diacetylene: Reactions with Benzene and Toluene†

Allison G. Robinson, Paul R. Winter, Christopher Ramos, and Timothy S. Zwier*

Department of Chemistry, Purdue University, West Lafayette, Indiana 47907-1393

Received: April 14, 2000; In Final Form: June 12, 2000

The reactions of metastable diacetylene with benzene and toluene are explored using a molecular beam pump−probe time-of-flight mass spectrometer. Diacetylene is laser-excited to the $2^1_0 6^1_0$ band of the $^1\Delta_u \leftarrow X^1\Sigma^+_g$ transition, whereupon rapid intersystem crossing occurs to the lowest triplet states. The triplet state diacetylene then reacts with either benzene or toluene as the gas mixture traverses a short reaction tube (∼20 μs). The reactions are quenched as the gas mixture expands into the ion source region of a time-of-flight mass spectrometer where the primary photoproducts are detected using vacuum ultraviolet (VUV) photoionization or resonant two-photon ionization (R2PI). The major products from the reaction of diacetylene and benzene have molecular formulas C_8H_6 and $C_{10}H_6$, and are identified as phenylacetylene and phenyldiacetylene using R2PI spectroscopy. The major products from metastable diacetylene's reaction with toluene are C_9H_8 and $C_{11}H_8$. The C_9H_8 product is confirmed as a mixture of *o*-, *m*-, and *p*-ethynyltoluene, with the ortho product dominating. Mechanisms for the formation of the above products are proposed based on deuterium substitution studies of the reactions. The potential importance of these reactions is discussed as they relate to hydrocarbon growth in sooting flames.

I. Introduction

Diacetylene (C_4H_2, H−C≡C−C≡C−H) is an important molecule in combustion chemistry. It is one of the most abundant C4 species found in sooting flames, particularly acetylene flames.[1−4] Diacetylene is also thought to play a role in the formation of aromatic molecules in flames, which lead to soot formation.[5,6] There are two main pathways in current models for benzene formation in flames. First, the radical/radical recombination of two propargyl radicals ($\dot{C}H_2$−C≡C−H) produces 1,5 hexadiyne (HC≡C$(CH_2)_2$C≡CH) which can subsequently isomerize to benzene.[4,7] Second, acetylene can react with an isomer of either C_4H_3 or C_4H_5 to produce C_6H_5 or C_6H_7, which can add or lose an H atom to form benzene. Both C_4H_3 and C_4H_5 are closely coupled with reactions either forming or depleting diacetylene.[8−10] We recently demonstrated the importance of the second pathway in forming benzene in methane flames doped with diacetylene and vinylacetylene.[11]

After the formation of the first aromatic ring, further growth to soot requires production of larger polycyclic aromatic hydrocarbons (PAHs). One of the proposed routes to formation of the second aromatic ring is the addition of acetylene to benzene through the hydrogen abstraction acetylene addition (HACA) mechanism.[5,8,12] Alternatively, recombination of cyclopentadienyl radicals (C_5H_5) is thought to be an efficient route to naphthalene.[8,13,14] Several other pathways have been proposed, including one in which diacetylene reacts with phenyl radical to form the naphthyl radical,[15] which could then abstract a hydrogen to give naphthalene. Further elucidation of the possible pathways to the formation of substituted aromatics and subsequently naphthalene or substituted naphthalenes and higher order ring structures[16,17] is important in determining suitable mechanisms for growth of PAHs in flames.

Diacetylene has a rich history of photochemical studies. Glicker and Okabe carried out one of the early studies on the photochemistry of diacetylene.[18] Among the important results of their work was the determination that following ultraviolet excitation, diacetylene reacts out of metastable triplet states and not via radical reactions. This molecular reactivity is a natural consequence of the strong bonds in diacetylene, which prevent radical formation following photoexcitation throughout much of the ultraviolet.[18] However, rapid polymerization in their bulb studies prevented the determination of primary products. We have studied the primary products of the reactions of metastable diacetylene with several small hydrocarbons,[19−23] but the present work marks the first study of its reactions with an aromatic molecule.

In seeking to understand the reactivity and importance of the triplet states of C_4H_2, further *spectroscopic* characterization of the triplet states themselves is needed. The electron energy loss spectra (EELS) of Allan identified two low-lying triplet states, $T_1(^3\Sigma_u^+)$ and $T_2(^3\Delta_u)$, which are likely candidates for the metastable state(s) responsible for the observed photochemistry.[24] We have recently recorded a singlet−triplet absorption spectrum of diacetylene in the 370 nm region using cavity ringdown spectroscopy, probing the transition assigned to the T_2 upper state, which is of $^3\Delta_u$ symmetry in the linear configuration.[25]

In this paper, we focus instead on the *chemistry* of the triplet state(s) of diacetylene. Recently, we demonstrated that the reaction of metastable diacetylene with 1,3-butadiene formed benzene and phenylacetylene, raising the prospect that such reactions could play a role in aromatic formation in flames.[23] Accordingly, we are interested in exploring whether diacetylene can play a role in forming larger fused aromatic rings. The present paper, therefore, analyzes the reactions of metastable diacetylene with benzene and toluene using the same laser pump−probe scheme used in earlier studies.[19−23,26]

II. Experimental Section

The experiments described in this paper were carried out in a molecular beam time-of-flight (TOF) mass spectrometer designed to study the primary products of photoinitiated

† Part of the special issue "C. Bradley Moore Festschrift".

* To whom correspondence should be addressed. Fax: (765) 494-0239. E-mail: zwier@purdue.edu.

10.1021/jp001427v CCC: $19.00
Published on Web 07/29/2000

reactions.[20] The gas handling system was modified in order to minimize the contact of the diacetylene with liquid benzene or toluene because we found that diacetylene reacts with liquid benzene to form polymeric products, while the two gas phase reactants do not react on the time scale of our experiment. Therefore, the reaction mixture was prepared by flowing helium at approximately 1 sccm over liquid benzene (toluene) in a stainless steel reservoir to pick up the sample at its vapor pressure (100 and 33 Torr, respectively). The concentration of benzene (toluene) in helium was approximately 5% (2%) at 20 psig backing pressure. The diacetylene (4−7% in helium) was introduced to the pulsed valve through a separate line, again at approximately 1 sccm flow. The two gas lines were combined just prior to the pulsed valve (R.M. Jordan Co.) and the mixture was pulsed into the chamber at 10 Hz.

In these experiments, it was important to avoid the photopolymerization reactions that diacetylene experiences under bulb conditions. The reactants were expanded into a short reaction tube (1 cm long, 2 mm i.d.) affixed to the pulsed valve. While the reactant mixture was in the tube, photochemistry was initiated using the doubled output (0.7 mJ/pulse) of a Nd:YAG pumped KTP/BBO optical parametric converter (LaserVision). The photoexcitation laser was tuned to the $2^1_0 6^1_0$ of the $^1\Delta_u \leftarrow X^1\Sigma^+_g$ transition in diacetylene (231.5 nm).[19] From the known absorption cross section of diacetylene (80 cm^{-1} atm^{-1}),[18] we estimate that 2−3% of the diacetylene was photoexcited by the ultraviolet laser. Rapid intersystem crossing occurs from the excited singlet state, either directly or mediated by the lower energy $^1\Sigma_u^+$ state, producing high vibrational levels of the low-lying triplet states ($^3\Delta_u$ and/or $^3\Sigma_u^+$).[18,20] Reactions then occur in parallel with vibrational deactivation in the triplet manifold. The 20 μs traversal of the gas mixture in the tube allows for sufficient collisions to initiate primary $C_4H_2^* + C_6H_6/C_7H_8$ chemistry, after which free expansion into the vacuum chamber quenches further reactions. The absence of larger photoproducts provides strong evidence that secondary reactions are of minor importance using this scheme.

The gas mixture was ionized approximately 7 cm downstream from the exit of the reaction tube in the extraction region of the TOF mass spectrometer using either vacuum ultraviolet (VUV) ionization or resonant two-photon ionization (R2PI). VUV photoionization achieves general mass analysis with minimal fragmentation using 118 nm (10.5 eV) light produced by tripling the third harmonic of a Nd:YAG laser in a xenon/argon gas mixture.[20,27] Alternatively, R2PI produces ultraviolet spectra of the products, which can be used in structural analysis. Scans over the wavelength ranges depicted in this work (570−480 nm) were taken using the doubled output of a Nd:YAG pumped dye laser in three dye regions (Coumarin 540A, 503, 480).

Benzene, deuterated benzene, toluene, and deuterated toluene were used as supplied (Fisher, 99.9%; Cambridge Isotope Laboratories, 99.6%; Fisher, 99.8%; Aldrich, 99%; respectively). Diacetylene and deuterated diacetylene were synthesized in our laboratory using previously described methods.[20,21] The phenyldiacetylene was synthesized using the method of Brandsma.[28] Due to the difficulty in isolating pure phenyldiacetylene, the synthesis was verified by comparison of the ultraviolet spectrum of the reaction mixture in methanol with a literature ultraviolet spectrum of phenyldiacetylene.[29] The *o*-ethynyltoluene was synthesized at Hampford Research, Inc.,[30] while the *m*- and *p*-ethynyltoluenes are available commercially (Lancaster, 99% and Aldrich, 97%).

III. Results

A. $C_4H_2^* + C_6H_6$ VUV Photoionization Studies. Figure 1a shows the difference mass spectrum from the reaction of a 1:1.3 mixture of diacetylene and benzene, as determined from the peak areas of the primary ions in the VUV mass spectra. The reported spectrum is the difference between a mass spectrum taken with the photoexcitation laser on and one taken with the photoexcitation laser off. The difference mass spectrum highlights the photochemical products of the reaction of metastable diacetylene with benzene. The molecular formulas in the figure were determined from the mass-to-charge ratios of the respective peaks.

The two reactant peaks, C_4H_2 ($m/z = 50$) and C_6H_6 ($m/z = 78$), are not shown in the figure. They are about 100−200 times larger than the photoproduct peaks, consistent with the small amount of diacetylene excited by the ultraviolet laser. A high voltage pulse (+800 V) is applied to a deflection plate, located early in the TOF tube, to deflect the reactant ions away from the microsphere plate so the photoproduct signals can be observed. Consequently, photoproducts with masses in the 45−80 amu range are not detected, although no such products are anticipated. Previous studies of polyyne, polyenyne, cumulene,[22] and aromatic molecules[23] have shown no evidence of fragmentation upon 118 nm ionization, consistent with other studies of a range of hydrocarbons.[31] Therefore, we assume throughout this paper that the species that appear in the difference mass spectra represent the nascent, neutral products formed in the gas phase reaction.

The two major photochemical product peaks observed for the $C_4H_2^* + C_6H_6$ reaction (Figure 1a) are $m/z = 102$ (C_8H_6) and $m/z = 126$ ($C_{10}H_6$) with $m/z = 127$ ($C_{10}H_7$) as a minor product.[32] The percent product yields are given in Table 1. The C_8H_2 and C_8H_3 products from the $C_4H_2^* + C_4H_2$ reaction also appear in Figure 1a, as this reaction occurs in competition with the reaction of interest. The relevant reactions are as follows:

$$C_4H_2^* + C_4H_2 \rightarrow C_6H_2 + (C_2H_2) \qquad k_{C_6H_2} \qquad (1a)$$

$$\rightarrow C_8H_2 + (H_2 \text{ or } 2H) \qquad k_{C_8H_2} \qquad (1b)$$

$$\rightarrow C_8H_3 + (H) \qquad k_{C_8H_3} \qquad (1c)$$

$$C_4H_2^* + C_6H_6 \rightarrow C_8H_6 + (C_2H_2) \qquad k_{C_8H_6} \qquad (2a)$$

$$\rightarrow C_{10}H_6 + (H_2 \text{ or } 2H) \qquad k_{C_{10}H_6} \qquad (2b)$$

$$\rightarrow C_{10}H_7 + (H) \qquad k_{C_{10}H_7} \qquad (2c)$$

The products listed in parentheses have ionization potentials greater than 10.5 eV, so they are not observable using 118 nm VUV photoionization. The C_6H_2 and C_8H_2 products from $C_4H_2^* + C_4H_2$ have been shown to be triacetylene and tetracetylene, respectively in an earlier work.[26] The C_6H_2 product is below the mass of benzene and therefore is pulsed away by the high voltage pulse.

In order to confirm that the photoproducts of the $C_4H_2^* + C_6H_6$ reaction were coming exclusively from photoexcited diacetylene, action spectra of the three photoproducts were recorded by tuning the photoexcitation laser through the $2^1_0 6^1_0$ transition of diacetylene while monitoring the relevant mass channels. All three products are formed following excitation of the diacetylene, producing action spectra (not shown) that mirror the absorption spectrum of diacetylene. Benzene has a small absorption ($6^1_0 1^5_0$) near the diacetylene $2^1_0 6^1_0$ transition, so

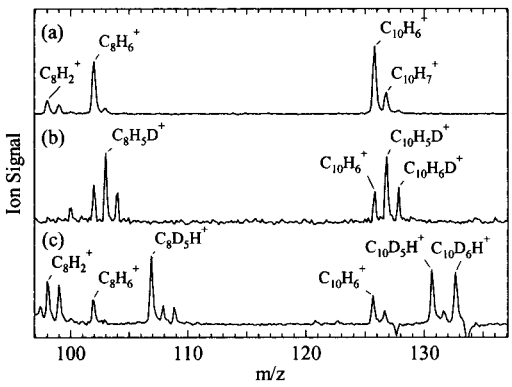

Figure 1. VUV photoionization difference mass spectra highlighting the photoproducts for the reactions (a) $C_4H_2^* + C_6H_6$, (b) $C_4D_2^* + C_6H_6$, and (c) $C_4H_2^* + C_6D_6$. The reactant mass peaks are 100−200 times larger than the photoproduct peaks and are not shown. Signal from the fully non-deuterated reaction is present in the two deuterated cases, due to residual non-deuterated sample in the gas handling system.

difference mass spectra were also taken at two other diacetylene transitions, the $2^2_0 6^1_0$ (220.7 nm) and the 6^1_0 (243.1 nm),[33] where there are no benzene absorptions. The data at the other two photochemistry wavelengths reproduced the products and intensity ratios shown in Figure 1a. The $2^1_0 6^1_0$ transition was used as the primary photoexcitation wavelength because it is the most intense diacetylene transition in the wavelength region well below the lowest dissociation threshold of C_4H_2.

One potential complication of the present study is the possibility that $C_4H_2^*$ could undergo triplet−triplet energy transfer to benzene, followed by the reaction of $C_6H_6^*$ with C_4H_2. While not a focus of the present study, we also observed C_8H_6 and $C_{10}H_6$ photoproducts from the $C_6H_6^* + C_4H_2$ reaction when benzene was excited via its 6^1_0 transition (259.15 nm). Under the laser power (∼0.7 mJ) and bandwidth (∼2 cm^{-1}) conditions of this experiment, we estimate that the photoexcitation laser excites no more than a few percent of the benzene molecules in the reaction tube. Following photoexcitation at the 6^1_0 transition, the benzene that does not fluoresce (18%)[34] predominantly intersystem crosses to the triplet manifold (63%).[35] The difference mass spectra recorded following excitation of C_6H_6 had a qualitatively different intensity ratio for the two primary products (∼2.5:1 $C_{10}H_6$:C_8H_6 in the benzene excitation case, as opposed to ∼1:1 $C_{10}H_6$:C_8H_6 in the case of diacetylene excitation). Furthermore, there was no evidence of $C_4H_2^* + C_4H_2$ reaction products when we excited the benzene rather than diacetylene. These findings suggest that triplet−triplet energy transfer in either direction does not compete effectively with direct reactions of the triplet state molecule. While the $C_6H_6^*$ chemistry is interesting in its own right, it is not pursued further here.

As in earlier studies,[20−23] reaction time scans were carried out to ensure that the observed photoproducts have arrival times consistent with primary, gas phase photoproducts uncompromised by wall reactions. In these scans, the VUV photoionization laser is fixed in time relative to the gas pulse while the timing of the photoexcitation laser is scanned. The products all appear in a symmetric, Gaussian-like distribution in time, with a full width at half-maximum (fwhm) of about 20 μs. They are peaked at an arrival time corresponding to their traversal from the reaction tube to the ion source region. The form of this distribution was the same for all of the $C_4H_2^* + C_6H_6$ and $C_4H_2^* + C_7H_8$ photoproducts.

In order to gain further insight into the structure of the photoproducts, deuterium isotope labeling studies were carried out. Figure 1b and c, shows the difference mass spectra for the $C_4D_2^* + C_6H_6$ and the $C_4H_2^* + C_6D_6$ reactions, respectively. Percent product yields for these reactions are given in Table 1. In the former reaction (Figure 1b), the mass of the two major photoproducts (C_8H_6 and $C_{10}H_6$) and the minor $C_{10}H_7$ product all increased by only one mass unit, consistent with one deuterium atom from C_4D_2 being retained in each photoproduct (C_8H_5D, $C_{10}H_5D$, and $C_{10}H_6D$).

$$C_4D_2^* + C_6H_6 \rightarrow C_8H_5D + (C_2HD) \quad (3a)$$

$$\rightarrow C_{10}H_5D + (HD \text{ or } H + D) \quad (3b)$$

$$\rightarrow C_{10}H_6D + (D) \quad (3c)$$

The exclusive formation of $C_{10}H_6D$ in reaction 3c shows that it is a diacetylenic hydrogen that is preferentially lost from the reaction complex.

The reaction of $C_4H_2^* + C_6D_6$ (Figure 1c) produces isotopic products consistent with those from $C_4D_2^* + C_6H_6$.

$$C_4H_2^* + C_6D_6 \rightarrow C_8D_5H + (C_2HD) \quad (4a)$$

$$\rightarrow C_{10}D_5H + (HD \text{ or } H + D) \quad (4b)$$

$$\rightarrow C_{10}D_6H + (H) \quad (4c)$$

As before, the C_8D_5H and $C_{10}D_5H$ products indicate that the deuterated benzene is contributing five deuterium atoms and the diacetylene one hydrogen to each product. The minor $C_{10}D_6H$ photoproduct also confirms that all of benzene's deuterium atoms are retained in this product.

B. $C_4H_2^* + C_6H_6$ Product R2PI Studies. The mass spectral data provides the molecular formulas of the photoproducts, but it cannot distinguish among the various possible isomers that could be produced. Therefore, R2PI spectra were taken of the C_8H_6 and $C_{10}H_6$ products. The R2PI spectrum of the C_8H_6 product is shown in Figure 2a, compared with the R2PI spectrum in the region of the $S_1 \leftarrow S_0$ origin of a known sample of phenylacetylene taken under similar conditions (Figure 2b).[23] The match between the two spectra positively identifies the C_8H_6 photoproduct as phenylacetylene.

The second major product, $C_{10}H_6$, could be any one of several possible isomers, including *o*-, *m*-, and *p*-diethynylbenzene and phenyldiacetylene.

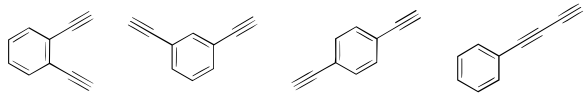

The R2PI spectrum of the $C_{10}H_6$ photoproduct is shown in Figure 3a. The spectrum shows only broad features of about 350 cm^{-1} fwhm, with hints of substructure beneath it, presenting a sharp contrast to the phenylacetylene spectrum in Figure 2. A gas phase UV−visible absorption spectrum was taken of the vapor above a known sample of phenyldiacetylene (Figure 3b). The broad features of the room-temperature ultraviolet absorption spectrum of the vapor above the phenyldiacetylene match the transitions in the $C_{10}H_6$ photoproduct R2PI spectrum, providing confirmation that the $C_{10}H_6$ photoproduct is phenyldiacetylene.

Attempts to record an R2PI spectrum from the known phenyldiacetylene were unsuccessful. The difficulties in obtaining this spectrum were likely the combined consequence of the problems with handling this compound and the modest vapor pressure of phenyldiacetylene in our impure sample. The

TABLE 1: Percent Product Yields[a,b] for Metastable Diacetylene Reacting with Benzene and Toluene and Their Corresponding Isotopic Reactions

C_4H_2* + C_6H_6		C_4D_2* + C_6H_6		C_4H_2* + C_6D_6		C_4H_2* + C_7H_8		C_4D_2* + C_7H_8		C_4H_2* + C_7D_8	
C_8H_6	39%	C_8H_5D	40%	C_8D_5H	38%	C_8H_6	4%	C_8H_5D	4%[c]	C_8D_5H	4%[c]
$C_{10}H_6$	48%	$C_{10}H_5D$	44%	$C_{10}D_5H$	31%	C_9H_8	42%	C_9H_7D	45%	C_9D_7H	25%
$C_{10}H_7$	13%	$C_{10}H_6D$	16%	$C_{10}D_6H$	31%	$C_{10}H_6$	5%	$C_{10}H_5D$	6%	$C_{10}D_5H$	8%
						$C_{11}H_8$	38%	$C_{11}H_7D$	34%	$C_{11}D_7H$	25%
						$C_{11}H_9$	11%	$C_{11}H_8D$	11%	$C_{11}D_8H$	38%

[a] Percent product yields were determined from the integrated peak areas in the difference mass spectrum. [b] Estimated error on the percent yields is ±3%. [c] This yield was not available due to interference from other features in the mass spectrum. The yield is assumed it to be the same as in the non-deuterated case.

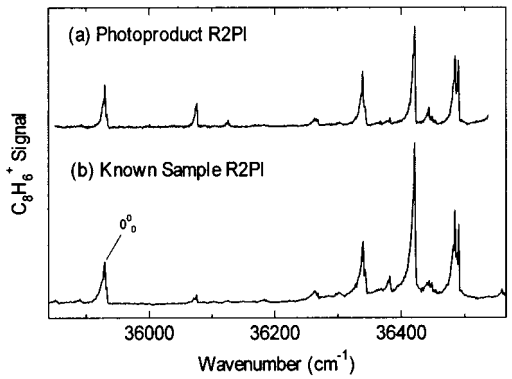

Figure 2. (a) One-color R2PI of the C_8H_6 photoproduct from C_4H_2* + C_6H_6. (b) R2PI spectrum of the $S_1 \leftarrow S_0$ origin region of phenylacetylene seeded in helium under similar conditions to those used for the photochemistry, identifying the C_8H_6 photoproduct from C_4H_2* + C_6H_6 as phenylacetylene (taken from ref 23).

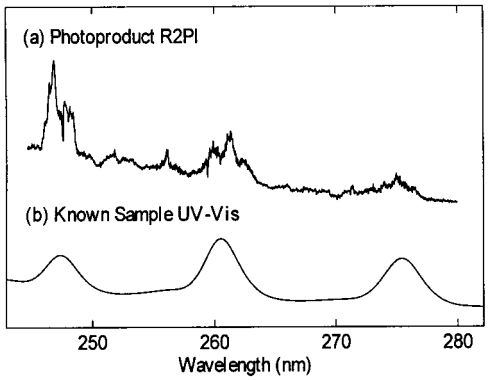

Figure 3. (a) One-color R2PI of the $C_{10}H_6$ photoproduct from C_4H_2* + C_6H_6, smoothed using a third-order boxcar function. (b) Ultraviolet absorption spectrum of gas phase phenyldiacetylene at room temperature.

inherent breadth of phenyldiacetylene's spectrum in the ultraviolet region suggests that fast nonradiative processes occur in its excited state. Similar fast, nonradiative processes are present in diacetylene's $S_2 \leftarrow S_0$ spectrum,[33] suggesting that the diacetylenic moiety is responsible for the fast, nonradiative processes in phenyldiacetylene. The long Franck−Condon progression that appears in the spectrum of phenyldiacetylene is due to the C≡C stretch (2053 cm^{-1}), and is similar to the corresponding progression in diacetylene's gas phase ultraviolet spectrum, but shifted about 30 nm to the red.

C. C_4H_2* + C_7H_8 VUV Photoionization Studies. In order to probe the effect that methyl substitution on an aromatic ring has on the diacetylene photochemistry, a similar set of experiments was carried out with toluene. Figure 4 shows a difference TOF mass spectrum of the photoproducts of the C_4H_2* + C_7H_8 reaction from a mixture containing a 1:1.1 ratio of diacetylene to toluene. The two major products are C_9H_8 (m/z = 116) and $C_{11}H_8$ (m/z = 140) with minor contributions from C_8H_6 (m/z = 102), $C_{10}H_6$ (m/z = 126), and $C_{11}H_9$ (m/z = 141). The major photoproducts differ from the corresponding products in the C_4H_2* + C_6H_6 reaction by 14 mass units, as would be anticipated if each product is a methyl-substituted version of its analogue in the benzene reaction. The relevant reactions are detailed below, listed in order of percent photoproduct yield (see Table 1).

$$C_4H_2^* + C_7H_8 \rightarrow C_9H_8 + (C_2H_2) \qquad k_{C_9H_8} \quad (5a)$$

$$\rightarrow C_{11}H_8 + (H_2 \text{ or } 2H) \qquad k_{C_{11}H_8} \quad (5b)$$

$$\rightarrow C_{11}H_9 + (H) \qquad k_{C_{11}H_9} \quad (5c)$$

$$\rightarrow C_{10}H_6 + (CH_4) \text{ or } CH_3 + (H) \qquad k_{C_{10}H_6} \quad (5d)$$

$$\rightarrow C_8H_6 + C_3H_4 \qquad k_{C_8H_6} \quad (5e)$$

Once again, the C_4H_2* + C_4H_2 reaction occurs in parallel with the C_4H_2* + C_7H_8 reaction, but these products are outside the mass range shown in Figure 4. As with the benzene reaction, action spectra and reaction time profiles were taken to confirm that the photoproducts were all coming from the excitation of gas phase diacetylene and that wall effects were negligible.

The reactions of C_4D_2* + C_7H_8 and C_4H_2* + C_7D_8 were also carried out (not shown). The percent product yields are included in Table 1. The results were consistent with what was observed in the deuterated benzene experiments, giving the following suite of reactions:

$$C_4D_2^* + C_7H_8 \rightarrow C_9H_7D + (C_2HD) \quad (6a)$$

$$\rightarrow C_{11}H_7D + (HD \text{ or } H + D) \quad (6b)$$

$$\rightarrow C_{11}H_8D + (D) \quad (6c)$$

$$\rightarrow C_{10}H_5D + (CH_3D) \text{ or } CH_3 + (D) \quad (6d)$$

$$\rightarrow C_8H_5D + C_3H_3D \quad (6e)$$

$$C_4H_2^* + C_7D_8 \rightarrow C_9D_7H + (C_2HD) \quad (7a)$$

$$\rightarrow C_{11}D_7H + (HD \text{ or } H + D) \quad (7b)$$

$$\rightarrow C_{11}D_8H + (H) \quad (7c)$$

$$\rightarrow C_{10}D_5H + (CD_3H) \text{ or } CD_3 + (H) \quad (7d)$$

$$\rightarrow C_8D_5H + C_3D_3H \quad (7e)$$

The deuterated toluene reaction results confirmed that the C_8H_6 and $C_{10}H_6$ products are indeed minor products of the toluene reaction and not simply products from a reaction of diacetylene with residual benzene in the system.

D. C_4H_2* + C_7H_8 Product R2PI Studies. On the basis of a comparison with the C_4H_2* + C_6H_6 reaction, one anticipates

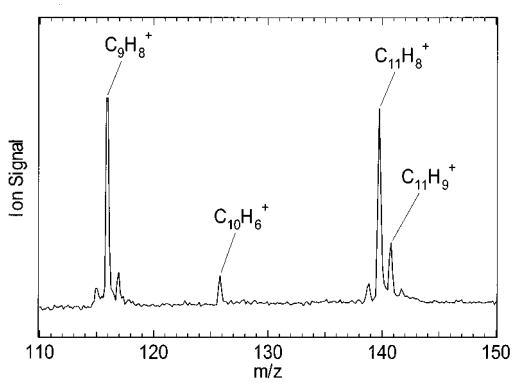

Figure 4. VUV photoionization difference mass spectrum highlighting the photoproducts for the reaction C_4H_2* + C_7H_8. The reactant mass peaks are 100−200 times larger than the photoproduct peaks and are therefore not shown. The minor product C_8H_6 is also not shown due to interference effects from an impurity.

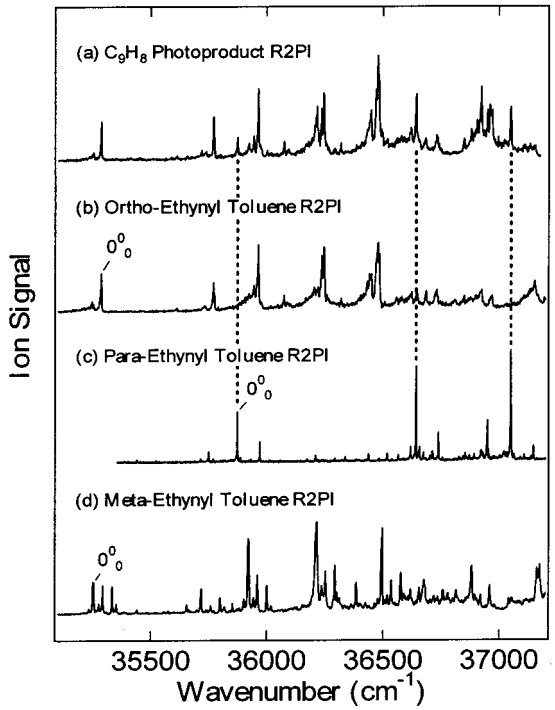

Figure 5. (a) One-color R2PI of the C_9H_8 photoproduct from C_4H_2* + C_7H_8. (b) R2PI spectrum of the $S_1 \leftarrow S_0$ origin region of *o*-ethynyltoluene seeded in helium under similar conditions to those used for the photochemistry. (c) R2PI spectrum of the $S_1 \leftarrow S_0$ origin region of *p*-ethynyltoluene seeded in helium under similar conditions to those used for the photochemistry. (d) R2PI spectrum of the $S_1 \leftarrow S_0$ origin region of meta-ethynyltoluene seeded in helium under similar conditions to those used for the photochemistry. Spectra in this figure are not power normalized.

the C_9H_8 photochemical product to be one or more of the three ethynyltoluene isomers (ortho, meta, and para). Indene and 3-phenyl-1-propyne are other possibilities consistent with the molecular formula.

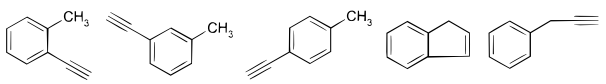

This range of potential products highlights the importance of having spectroscopic information to aid in positive identification of the structure(s) of the products.

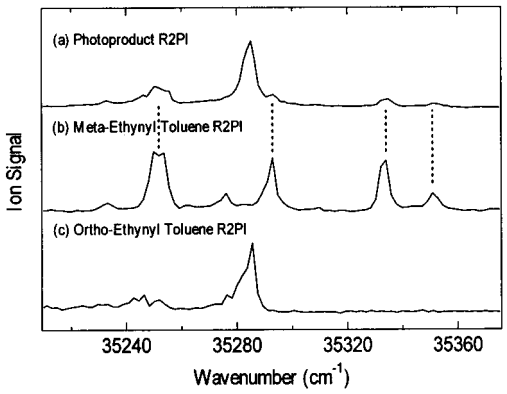

Figure 6. Blow up of the one-color R2PI of the (a) C_9H_8 photoproduct from C_4H_2* + C_7H_8, (b) *m*-ethynyltoluene, and (c) *o*-ethynyltoluene over the origin region.

The R2PI spectrum of the photochemical product in the 268−285 nm region is shown in Figure 5a. Indene was removed as a candidate based on a comparison with a literature R2PI spectrum.[36] The R2PI spectrum of 3-phenyl-1-propyne (Aldrich, 97%) also was not a match with the observed photochemical product. The R2PI spectra of the three ethynyltoluene isomers are shown in Figure 5b−d. The C_9H_8 photochemical product spectrum (Figure 5a) contains transitions readily assignable to both *o*- and *p*-ethynyltoluene isomers. Figure 6a shows a blow up of the photoproduct spectrum around the origin region of the ortho and meta isomers, while Figure 6b and c shows the corresponding *m*- and *o*-ethynyltoluene spectra over the same region. The one-to-one correspondence between several of the weak features in the photoproduct spectrum with the *m*-ethynyltoluene transitions identifies the meta isomer as also present in the photoproduct spectrum. In order to quantify the amount of *o*- and *p*-ethynyltoluene in the photoproduct, a spectrum was recorded of a known mixture of the ortho and para isomers. Ratios were taken of peak areas from that spectrum to their corresponding peaks in the photoproduct spectrum, and it was determined that the photoproduct represents a 4.9(±1.8):1 mixture of *o*- to *p*-ethynyltoluene. Due to the weak intensity of the meta transitions in the photoproduct, no attempt was made to quantify its yield relative to the other isomers.

Attempts to record an R2PI spectrum of the $C_{11}H_8$ photoproduct produced a weak signal with insufficient intensity to make any clear structural deductions. However, the resonantly enhanced signal occurs in the same wavelength region as phenyldiacetylene, suggesting that this product is the analogous diethynyltoluene. On the basis of a comparison with the C_9H_8 photoproduct, one might anticipate that $C_{11}H_8$ is a mixture of the ortho, meta, and para isomers. However, given the difficulties encountered in preparing the phenyldiacetylene sample, no efforts were made to synthesize any of the diethnyltoluene isomers, and no positive structural identification was made. In addition, no attempts were made to record R2PI spectra of the minor photoproducts.

IV. Discussion

A. Percent Product Yields. The percent product yields extracted from the difference TOF mass spectra are given in Table 1; analogous sets of products dominate in all circumstances ($C_8H_{6-x}D_x$ and $C_{10}H_{6-x}D_x$ for the benzene reaction, $C_9H_{8-x}D_x$ and $C_{11}H_{8-x}D_x$ for the toluene reaction). In fact, the distributions of products both between the two reactions and between those formed from non-deuterated and deuterated reactants are consistent throughout. The only exceptions are the

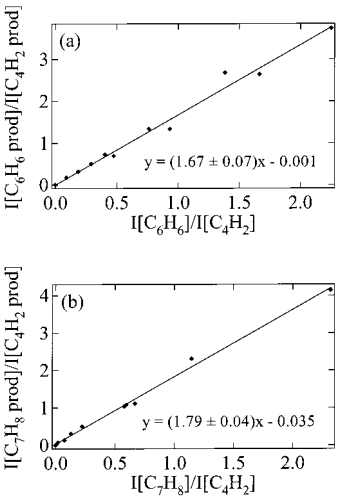

Figure 7. (a) Concentration study for the reaction $C_4H_2^* + C_6H_6$. Plotted are the ratio of product ion intensities $I[C_6H_6$ products$]/I[C_4H_2$ products] versus the ratio of reactant ion intensities $I[C_6H_6]/I[C_4H_2]$. The slope of the line fit to these points gives the relative rate constant for the reaction, $k_{C_6H_6}/k_{C_4H_2} = 1.67$. (b) Concentration study for the reaction $C_4H_2^* + C_7H_8$. Plotted are the ratio of product ion intensities $I[C_7H_8$ products$]/I[C_4H_2$ products] versus the ratio of reactant ion intensities $I[C_7H_8]/I[C_4H_2]$. The slope of the line fit to these points gives the relative rate constant for the reaction $k_{C_7H_8}/k_{C_4H_2} = 1.79$.

minor $C_{10}D_6H$ and $C_{11}D_8H$ products from the $C_4H_2^* + C_6D_6$ and $C_4H_2^* + C_7D_8$ reactions, respectively. These two products are increased in yield significantly relative to their nondeuterated analogues. We will return to this point following a consideration of the energetics of the various product channels in section C.

In order to extract quantitatively accurate quantum yields for the products from the data in Table 1, one would need to correct the observed ion signal for differences in absolute photoionization efficiencies at 118 nm. However, such data are not available, so we instead rely on the fact that the observed photoproducts are chemically similar in structure (e.g., phenylacetylene and phenyldiacetylene) and therefore are expected to have similar photoionization cross sections. On this basis, we assume that the photoion signals in Table 1 faithfully reflect the neutral product yields, recognizing the need for a quantitative determination in the future.

B. Relative Rate Constants. The metastable diacetylene reactions are carried out under early-time conditions in which secondary reactions are negligible. As we have shown in previous work, under similar conditions the results of a concentration study can be used to extract an effective rate constant for the reaction of interest relative to that for $C_4H_2^* + C_4H_2$, which occurs in parallel.[22] Within this pseudo-first-order kinetic model, which assumes similar photoionization cross sections for all species, a plot of the integrated intensity ratio of the product ion intensities from the $C_4H_2^* + C_6H_6$ (C_7H_8) reaction to those from the $C_4H_2^* + C_4H_2$ reaction versus the integrated intensity ratio of the benzene (toluene) to diacetylene primary ion signals should produce a linear plot with a slope equal to the rate constant ratio.

Figure 7a and b shows such plots for the $C_4H_2^* + C_6H_6$ and $C_4H_2^* + C_7H_8$ reactions. The linearity of both plots is consistent with the simple kinetic model used. The rate constant ratios obtained are $k_{C_6H_6}/k_{C_4H_2} = 1.67 \pm 0.07$ and $k_{C_7H_8}/k_{C_4H_2} = 1.79 \pm 0.04$, where the error bars represent 1 standard deviation of the mean. As expected, the relative rate constants for the reaction of metastable diacetylene with the two aromatics studied are quite similar. These rate constants are also appreciably larger than those previously obtained in studies of $C_4H_2^*$ reactions with small, aliphatic hydrocarbons.[20−23] Therefore, it is reasonable to assume that the increased collisional cross section of the larger species is more likely to be responsible for the increased rate rather than any reactant specific dynamic effect.

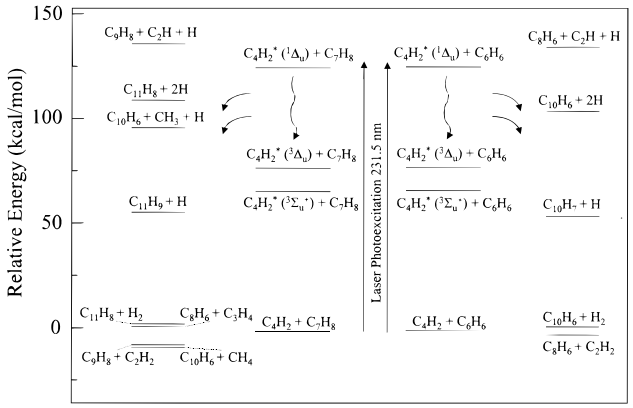

Figure 8. Thermodynamic energetics for the reactions $C_4H_2^* + C_6H_6$ and $C_4H_2^* + C_7H_8$. See Table 3 for more detail.

TABLE 2: Heats of Formation for the Various Photoproducts

species	ΔH_f (kcal/mol) at 298 °C	ref
H	52.103 ± 0.001	40
H_2	0	
C_2H	135.1 ± 0.7	40
C_2H_2	54.35 ± 0.19	41
CH_3	35.0 ± 0.1	40
CH_4	−17.8 ± 0.1	42
C_3H_4 (propyne)	44.32 ± 0.21	43
C_4H_2 (diacetylene)	111 ± 2	44
C_6H_6 (benzene)	19.7 ± 0.2	40
C_7H_8 (toluene)	12.0 ± 0.1	45
C_8H_6 (phenylacetylene)	73.27 ± 0.41	46
C_9H_8 (*o*-ethynyltoluene)	71 ± 3	47
$C_{10}H_6$ (phenyldiacetylene)	133 ± 3	47
$C_{11}H_8$ (*o*-diethynyltoluene)	126 ± 3	47

TABLE 3: Heats of Reaction for the Various Photoproduct Reactions

reaction[a,b]	ΔH_{rxn} (kcal/mol) at 298 °C
$C_4H_2 + h\nu(231.5\text{ nm}) \rightarrow C_4H_2^*$	123.5
$C_4H_2 + C_6H_6 \rightarrow C_8H_6 + (C_2H + H)$	130 ± 2
$C_4H_2 + C_6H_6 \rightarrow C_8H_6 + (C_2H_2)$	−3 ± 2
$C_4H_2 + C_6H_6 \rightarrow C_{10}H_6 + (H_2)$	2 ± 6
$C_4H_2 + C_6H_6 \rightarrow C_{10}H_6 + (2H)$	106 ± 6
$C_4H_2 + C_6H_6 \rightarrow C_{10}H_7 + (H)$	54 ± 6
$C_4H_2 + C_7H_8 \rightarrow C_8H_6 + C_3H_4$	−5 ± 2
$C_4H_2 + C_7H_8 \rightarrow C_9H_8 + (C_2H + H)$	135 ± 7
$C_4H_2 + C_7H_8 \rightarrow C_9H_8 + (C_2H_2)$	2 ± 6
$C_4H_2 + C_7H_8 \rightarrow C_{10}H_6 + CH_3 + (H)$	97 ± 6
$C_4H_2 + C_7H_8 \rightarrow C_{10}H_6 + (CH_4)$	−8 ± 6
$C_4H_2 + C_7H_8 \rightarrow C_{11}H_8 + (H_2)$	3 ± 6
$C_4H_2 + C_7H_8 \rightarrow C_{11}H_8 + (2H)$	107 ± 6
$C_4H_2 + C_7H_8 \rightarrow C_{11}H_9 + (H)$	55 ± 6

[a] The products listed in parentheses are not directly detected in the present work. [b] The product structures are those indicated in Table 2.

C. Energetics of the Reactions. Figure 8 is a schematic of the energetics for the diacetylene + benzene and diacetylene + toluene reactions. The heats of formation for the various photoproducts are listed in Table 2, while Table 3 gives the numerical values for the heats of reaction relative to the two ground state reactant molecules. Diacetylene is excited to the

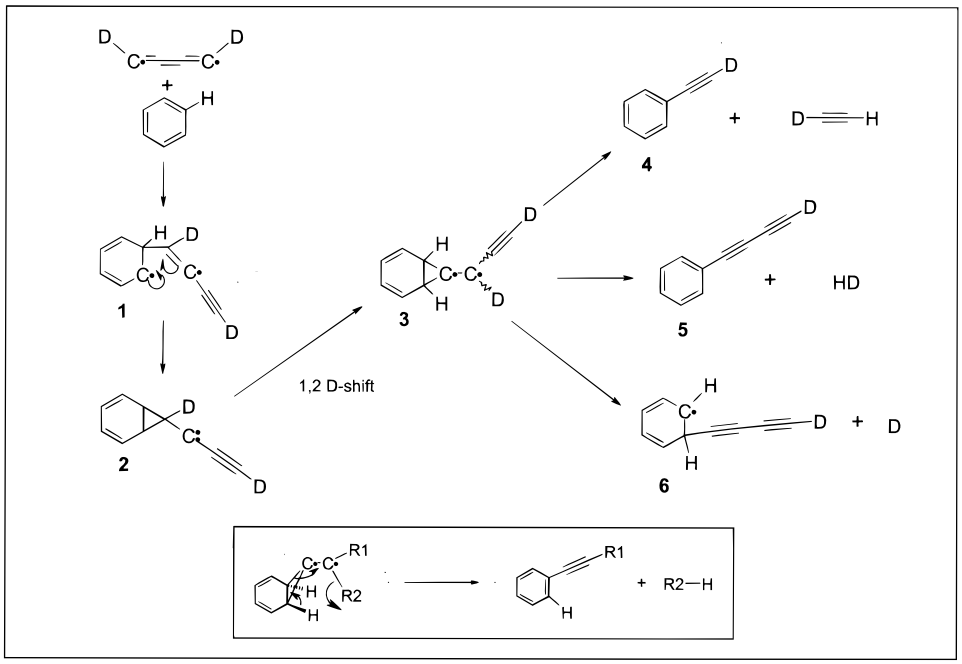

Figure 9. Proposed mechanism for the formation of phenylacetylene, phenyldiacetylene, and $C_{10}H_7$ radical species from $C_4H_2^* + C_6H_6$. The inset shows the details for the bond rearrangement of **3** to give the major reaction products. The triplet/singlet conversion may happen during the elimination, or triplet products may be formed (see text). The present experiment cannot distinguish at what point in the reaction the crossing occurs.

$2_0^1 6_0^1$ level of the $^1\Delta_u$ state providing 123.5 kcal/mol of energy above the ground state reactants, but the precise energy available for reaction depends on the degree of vibrational deactivation in the triplet manifold.

Due to the large C−H bond strength of C_2H_2, the C_8H_6 and C_9H_8 products can only be formed in conjunction with intact C_2H_2. On the other hand, $C_{10}H_6$ and $C_{11}H_8$ products can be formed with loss of either H_2 of 2H, depending on the degree of vibrational deactivation of $C_4H_2^*$. On the basis of the energetics of the two product channels, one would anticipate that loss of H_2 is preferred, but the present experiment cannot distinguish between those two pathways.

Since the minor products $C_{10}H_7$ and $C_{11}H_9$ are observed, some of the reaction complexes do lose a single hydrogen atom under the conditions of our experiment. If the $C_{10}H_7$ or $C_{11}H_9$ products have enough internal energy to fragment on a time scale fast by comparison to its collisional stabilization, they could then lose a second hydrogen to form the $C_{10}H_6$ or $C_{11}H_8$ product. In a previous study of the $C_4H_2^* + C_4H_2$ reaction, the ratio of intensities of the C_8H_2 to C_8H_3 products (involving loss of H_2/2H or H, respectively) shifted toward C_8H_3 when the buffer gas used in the reaction was nitrogen as opposed to helium.[20] The nitrogen buffer serves as a more effective collisional deactivator than helium. If a similar competition prevails in the present case, it would provide a potential explanation for the anomalous increases in $C_{10}D_6H$ and $C_{11}D_8H$ products from the $C_4H_2^* + C_6D_6$ and $C_4H_2^* + C_7D_8$ reactions noted previously. This increase could indicate that the time scale for further fragmentation is slower when a deuterium atom on the aromatic is lost from the reaction complex, and therefore deactivation occurs before the second atom is ejected.

Finally, it should be noted that two of the minor channels from the diacetylene plus toluene reaction, namely the $C_8H_6 + C_3H_4$ and $C_{10}H_6 + CH_4$ product channels, have similar heats of reaction to the $C_9H_8 + C_2H_2$ and $C_{11}H_8 + H_2$ product channels, yet they clearly are not formed in comparable quantities. We ascribe this difference to mechanistic effects as will be discussed in the next section.

In spite of the degree of exothermicity of the reaction, the R2PI spectra of the photoproducts show very little internal energy. The spectra, particularly of the phenylacetylene and the *o*-ethynyltoluene, mimic the jet-cooled known sample spectra. It appears that the cooling which accompanies the expansion of the reaction mixture as it leaves the reaction tube is sufficient to remove most of the internal energy in the nascent products. This cooling simplifies the R2PI spectra of the products, but eliminates the possibility of learning anything about the reaction mechanism from the internal excitation observed in the products. Previously, the rotational energy of the benzene photoproduct in the $C_4H_2^* + C_4H_6$ reaction was estimated from the rotational band contour to be in the 50−100 K temperature range.[23]

D. Reaction Mechanisms. There are three key experimental findings that a mechanism must justify to explain the reaction of metastable diacetylene plus benzene or toluene within a similar framework. First, the major photoproducts in both the benzene reaction (C_8H_6 and $C_{10}H_6$) and in the toluene reaction (C_9H_8 and $C_{11}H_8$) were formed with similar propensities, suggesting that they arise from a common intermediate. Second, the loss of C_2H_2 or C_2HD must happen in a concerted fashion from the reaction complex. An analogous concerted loss of H_2 or HD seems plausible as well. The deuterium labeling experiments prove that one hydrogen must come from the diacetylene and the other from the benzene or toluene molecule. Finally, the mechanism must account for the observed distribution of *o*-, *m*-, and *p*-ethynyltoluene isomers formed in the $C_4H_2^* + C_7H_8$ reaction.

A mechanism that meets the above criteria is shown for the two reactions in Figures 9 and 10. The mechanisms presented use $C_4D_2^*$ rather than $C_4H_2^*$ as the reactant in order to distinguish the benzene and diacetylene hydrogens, and the triplet state diacetylene is represented as a cumulene diradical, as the calculations of Karpfen and Lischka[37] and Vila et al.[38] have suggested. For the $C_4D_2^* + C_6H_6$ reaction, initial attack of the cumulene diradical on a double bond of benzene produces **1**. Subsequently, the ortho radical center attacks the double bond in the carbon chain, resulting in ring closure and the triplet,

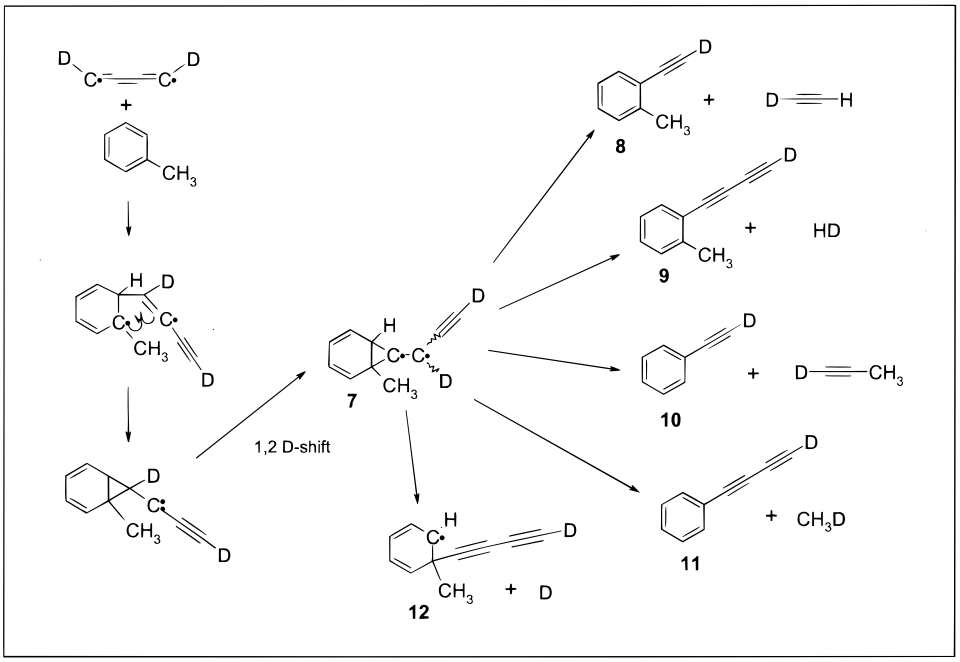

Figure 10. Proposed mechanism for the formation of *o*-ethynyltoluene, *o*-diethynyltoluene, phenylacetylene, phenyldiacetylene, and $C_{11}H_9$ radical species from C_4H_2* + C_7H_8.

bicyclic carbene **2**. A 1,2-deuterium shift then produces the key triplet diradical intermediate **3**. This intermediate can undergo a six-electron elimination to generate phenylacetylene (**4)** or phenyldiacetylene (**5)** with equal likelihood, or it can eliminate a single hydrogen to produce the $C_{10}H_7$ radical (**6)**. We favor a mechanism that proceeds on a triplet surface through to intermediate **3** for two reasons. First, the 1,2-deuterium shift may proceed more readily in the triplet carbene than on a singlet manifold. Second, the bent triplet state of **3** brings the ring hydrogen close to the end of the carbon chain for the elimination step. The inset of Figure 9 shows in detail the ene rearrangement that **3** undergoes to generate the major products, where R1 and R2 can represent either a hydrogen or an acetylene unit. It should be noted that some triplet state products could be formed in the elimination step, particularly triplet phenylacetylene. However, the detection of ground state phenylacetylene in R2PI spectroscopy indicates either that a spin crossing occurs during the elimination step or that the product undergoes intersystem crossing during the expansion.

An analogous mechanism accounts for the observed toluene products as well, with additional consideration of the possible sites for the cumulene radical attack. The attack on the ortho position is shown in Figure 10, as it produces the major fraction of the products. Following initial attack, the C_4H_2* + C_7H_8 mechanism proceeds via the same route as the benzene mechanism to the key intermediate **7**, which can undergo elimination via one of several pathways leading to *o*-ethynyltoluene (**8)**, *o*-diethynyltoluene (**9**), phenylacetylene (**10**), phenyldiacetylene (**11**), or the $C_{11}H_9$ radical species (**12**), all of which are observed experimentally.

The position of attack determines the distribution of isomers formed for both the $m/z = 116$ and $m/z = 140$ photoproducts. Methyl substitution on the ring favors cumulene diradical attack at ortho and para sites. An ipso attack would also produce a resonantly stabilized radical intermediate. Both ortho and ipso attacks would give intermediate **7** leading to ortho-substituted products. A para attack would produce an intermediate with the cyclopropane ring bridging the para and meta sites. One would expect this intermediate to eliminate with equal proclivity for formation of either para- or meta-substituted products. Note that para attack cannot lead to the formation of the C_8H_6 and $C_{10}H_6$ products, as the methyl group is too far removed to be involved in a concerted elimination reaction to form propyne or methane.

The proposed mechanism thus accounts for the distribution of *o*- to *p*-ethynyltoluene observed in the photoproduct spectrum. There are three attack sites, two ortho and one ipso, all of which produce ortho-substituted products, while there is only one para attack site, which produces meta- and para-substituted isomers in equal quantities. These statistics suggest that the photoproducts would be formed with a 6:1:1 ratio of ortho*:*para*:*meta substitution. The 4.9($\pm$1.8):1 ratio of *o*- to *p*-ethynyltoluene observed in the photoproduct spectrum is consistent with this effect, though other factors may also contribute to the observed product ratio. The mechanism predicts equal populations of para and meta isomers in the photoproducts. However, the meta origin is spread out over several torsional bands, resulting in weak meta transitions in the photoproduct spectrum, while the para isomer origin is a single band (see Figure 5).

The reaction mechanism in Figures 9 and 10 hinges on the unique properties of reaction intermediates **3** and **7**. Estimates of the heats of formation of the triplet state intermediates **3** and **7** ($\sim$50 kcal/mol above ground state reactants) place them at accessible energies in the C_4H_2* + benzene (toluene) reactions.[39] These intermediates provide a common framework for concerted loss of C_2HD and HD to form the two main products of each of the reactions with their correct isotopic compositions. The similar propensities of these products arises naturally from the cyclopropyl bond broken in **3** or **7** during the elimination of C_2HD and HD to form products. The mechanism also explains the observed ratio for the *o*- to *p*-ethynyltoluene products. Finally, intermediates **3** and **7** can account in a similar way for the formation of even minor products, particularly the formation of the C_8H_6 and $C_{10}H_6$ products from the toluene reaction by loss of CH_4 and C_3H_4, respectively, from intermediate **7**. These species may show up only as minor products due to a greater activation barrier for the elimination of a methyl, as opposed to a hydrogen, from the reaction complex.

E. Implications for Flame Chemistry. The importance of metastable C_4H_2 reactions in flame chemistry is not yet established. Spectroscopic signatures for C_4H_2* are needed before measurements of its concentration in flames can be carried out. Furthermore, absolute rate constants for its electronic quenching and chemical reaction are not yet available. Nevertheless, it is interesting at this early stage to note the types of products that are formed in these reactions in the context of flame chemistry. The reaction of metastable diacetylene with benzene forms phenylacetylene and phenyldiacetylene products that are similar in kind to those produced by the HACA mechanism. Yet, in bypassing free-radical formation, they constitute reaction pathways with unusually low energetic thresholds, which thereby deserve further investigation. Additionally, the preferential formation of *o*-ethnyltoluene in the reaction of metastable diacetylene with toluene is interesting in light of the heightened efficiency with which ortho-substituted aromatic rings form naphthalene in flames.[8]

Acknowledgment. The authors gratefully acknowledge the Department of Energy, Office of Basic Energy Sciences, Division of Chemical Sciences, for their support of this research under Grant No. DE-FG02-96ER14656. A.G.R. is grateful for fellowships from Purdue Research Foundation and Lubrizol Corp. The authors also acknowledge Professors John Grutzner and Rudolph Winter for the many useful discussions on reaction mechanisms. Finally, the authors are indebted to Stephen Finson of Hampford Research, Inc. for providing us with the *o*-ethynyltoluene sample, and to Professor Jillian Buriak and Michael Stewart of Purdue University for synthesizing the phenyldiacetylene.

References and Notes

(1) Bastin, E.; Delfau, J.-L.; Reuillon, M.; Vovelle, C.; Warnatz, J. *Symp. (Int.) Combust. [Proc.], 22nd* **1988**.

(2) Lam, F. W.; Howard, J. B.; Longwell, J. P. *Symp. (Int.) Combust. [Proc.], 22nd* **1988**, 323.

(3) Melius, C. F.; Miller, J. A.; Evleth, E. M. *Symp. (Int.) Combust. [Proc.], 24th* **1992**, 621.

(4) Miller, J. A.; Melius, C. F. *Combust. Flame* **1992**, *91*, 21.

(5) McEnally, C. S.; Pfefferle, L. D. *Combust. Sci. Technol*. **1997**, *128*, 257.

(6) McEnally, C. S.; Pfefferle, L. D. *Combust. Flame* **1998**, *115*, 81.

(7) Leung, K. M.; Lindstedt, R. P. *Combust. Flame* **1995**, *102*, 129.

(8) Marinov, N. M.; Pitz, W. J.; Westbrook, C. K.; Castaldi, M. J.; Senkan, S. M. *Combust. Sci. Technol*. **1996**, *116*, 211.

(9) Westmoreland, P. R.; Dean, A. M.; Howard, J. B.; Longwell, J. P. *J. Phys. Chem.* **1989**, *92*, 8171.

(10) Lindstedt, R. P.; Skevis, G. *Combust. Sci. Technol*. **1997**, *125*, 73.

(11) McEnally, C. S.; Robinson, A. G.; Pfefferle, L. D.; Zwier, T. S. *Combust. Flame*, in press.

(12) Wang, H.; Frenklach, M. *J. Phys. Chem.* **1994**, *98*, 11465.

(13) Melius, C. F.; Colvin, M. E.; Marinov, N. M.; Pitz, W. J.; Senkan, S. M. *Symp. (Int.) Combust. [Proc.], 26th* **1996**, 685.

(14) Castaldi, M. J.; Marinov, N. M.; Melius, C. F.; Huang, J.; Senkan, S. M.; Pitz, W. J.; Westbrook, C. K. *Symp. (Int.) Combust. [Proc.], 26th* **1996**, 693.

(15) Hausmann, M.; Homann, K.-H. *Ber. Bunsen-Ges. Phys. Chem.* **1997**, *101*, 651.

(16) Bapat, J. B.; Brown, R. F. C.; Bulmer, G. H.; Childs, T.; Coulston, K. J.; Eastwood, F. W.; Taylor, D. K. *Aust. J. Chem.* **1997**, *50*, 1159.

(17) Necula, A.; Scott, L. T. *J. Am. Chem. Soc.* **2000**, *122*, 1548.

(18) Glicker, S.; Okabe, H. *J. Phys. Chem.* **1987**, *91*, 437.

(19) Bandy, R. E.; Lakshminarayan, C.; Frost, R. K.; Zwier, T. S. *Science* **1992**, *258*, 1630.

(20) Bandy, R. E.; Lakshminarayan, C.; Frost, R. K.; Zwier, T. S. *J. Chem. Phys.* **1993**, *98*, 5362.

(21) Frost, R. K.; Zavarin, G.; Zwier, T. S. *J. Phys. Chem.* **1995**, *99*, 9408.

(22) Frost, R. K.; Arrington, C. A.; Ramos, C.; Zwier, T. S. *J. Am. Chem. Soc.* **1996**, *118*, 4451.

(23) Arrington, C. A.; Ramos, C.; Robinson, A. D.; Zwier, T. S. *J. Phys. Chem. A* **1998**, *102*, 3315.

(24) Allan, M. *J. Chem. Phys*. **1984**, *80*, 6020.

(25) Hagemeister, F. C.; Arrington, C. A.; Giles, B. J.; Quimpo, B.; Zhang, L.; Zwier, T. S. Cavity Ringdown methods for studying intramolecular and intermolecular dynamics. In *Cavity-Ringdown Spectroscopy—A New Technique for Trace Absorption Measurements*; Busch, K. J., Busch, M. A., Eds.; American Chemical Society: Washington, DC, 1999.

(26) Arrington, C. A.; Ramos, C.; Robinson, A. D.; Zwier, T. S. *J. Phys. Chem. A* **1999**, *103*, 1294.

(27) Mahon, R.; McIlrath, T. J.; Myerscough, V. P.; Koopman, D. W. *IEEE J. Quant. Electron*. **1979**, *6*, 444.

(28) Brandsma, L. *Preparative Acetylenic Chemistry*; Elsevier Publishing Co.: New York, 1988.

(29) Eastmond, R.; Walton, D. R. M. *Tetrahedron* **1972**, *28*, 4591.

(30) The synthetic procedure started with *o*-methylstyrene which was brominated to give the dibromo compound. Base-catalyzed elimination of Br_2 yielded the desired *o*-ethynyltoluene. The procedure was verified by the positive identification of *p*-ethynyltoluene synthesized from *p*-methylstyrene. The synthesis was performed by Stephen L. Finson at Hampford Research, Inc.

(31) Arps, J. H.; Chen, C. H.; McCann, M. P.; Datskou, I. *Appl. Spectrosc*. **1989**, *43*, 1211.

(32) Under certain experimental conditions, a photoproduct ion signal is also observed around $m/z = 91$ (C_7H_7, not shown in Figure 1). The photoion signal remains with full intensity when xenon is removed from the tripling cell, indicating that this product is ionized exclusively by the 355 nm light (~10 mJ/pulse) that also traverses the ion source region along with the 118 nm light. No ion signal was observed at the calibrated arrival time for $m/z = 91$ arising from VUV light, indicating that it is an insignificant product. The mass 91 signal has a greater than first-order power dependence with 355 nm light, suggesting that the product appears only by virtue of its low two-photon ionization threshold. The C_7H_7 species is likely to be tropyl radical, which has an ionization potential (6.28 eV) [Koenig, T.; Chang, J. C. *J. Am. Chem. Soc.* **1978**, *100*, 2240] accessible by two-photon, 355 nm ionization (6.985 eV) , as opposed to benzyl radical (IP = 7.2487 eV) [Berkowitz, J.; Ellison, G. B.; Gutman, D. *J. Phys. Chem*. **1994**, *98*, 2744].

(33) Bandy, R. E.; Lakshminarayan, C.; Zwier, T. S. *J. Phys. Chem.* **1992**, *96*, 5337.

(34) Noyes, W. A., Jr.; Mulac, W. A.; Harter, D. A. *J. Chem. Phys*. **1966**, *44*, 2100.

(35) Cundall, R. B.; Davies, A. S. *Trans. Faraday Soc*. **1966**, *62*, 1151.

(36) Kendler, S.; Zilberg, S.; Haas, Y. *Chem. Phys. Lett*. **1995**, *242*, 139.

(37) Karpfen, A.; Lischka, H. *Chem. Phys*. **1986**, *102*, 91.

(38) Vila, F.; Borowski, P.; Jordan, K. D., submitted for publication

(39) Benson, S. *Thermochemical Kinetics*, 2nd ed.; John Wiley & Sons: New York, 1976. Heats of formation were estimated using Benson's method of group additivity for the singlet ground state species. A factor of 2 eV was then added to account for the singlet−triplet splitting.

(40) Berkowitz, J.; Ellison, G. B.; Gutman, D. *J. Phys. Chem.* **1994**, *98*, 2744.

(41) Gurvich, L. V.; Veyts, I. V.; Alcock, C. B.; Iorish, V. S. *Thermodynamic Properties of Individual Substances*, 4th ed.; Hemisphere: New York, 1991; Vol. 2.

(42) Pittam, D. A.; Pilcher, G. *J. Chem. Soc., Faraday Trans. 1* **1972**, *68*, 2224.

(43) Wagman, D. D.; Kilpatrick, J. E.; Pitzer, K. S.; Rossini, F. D. *J. Res. Natl. Bur. Stand.* **1945**, *35*, 467.

(44) Stein, S. E.; Fahr, A. *J. Phys. Chem.* **1985**, *89*, 3714.

(45) Pedley, J. B.; Naylor, R. D.; Kirby, S. P. *Thermochemical Data of Organic Compounds*, 2nd ed.; Chapman & Hall, Ltd.: London, 1986.

(46) Davis, H. E.; Allinger, N. L.; Rogers, D. W. *J. Org. Chem.* **1985**, *50*, 3601.

(47) Benson, S. W. *Thermochemical Kinetics*, 2nd ed.; John Wiley & Sons: New York, 1976. Heats of formation for compounds for which no literature value could be found were estimated using Benson's method of group additivity. Benson provides no group values for $C_t-(C_t)$ or $C-(C_B)-(H)_3$, so the groups $C_t-(C)$ and $C-(C)(H)_3$ were used instead. The uncertainties listed represent estimates.